Supporting Information

Unraveling the charge storage mechanism of $Ti_3C_2T_x$ MXene electrode in acidic electrolyte

Hui Shao[1,2,†], Kui Xu[3,†], Yih-Chyng Wu[1,2], Antonella Iadecola[2], Liyuan Liu[1,2], Hongyun Ma[4], Liangti Qu[4], Encarnacion Raymundo-Piñero[2,5], Jixin Zhu[3], Zifeng Lin[6], Pierre-Louis Taberna[1,2], Patrice Simon[1,2,7,*]

[1] CIRIMAT, Université Paul Sabatier, CNRS, 31062 Toulouse, France

[2] Réseau sur le Stockage Electrochimique de l'Energie (RS2E), FR CNRS 3459, France

[3] Key Laboratory of Flexible Electronics (KLOFE) & Institute of Advanced Materials (IAM), Jiangsu National Synergetic Innovation Center for Advanced Materials (SICAM), Nanjing Tech University (NanjingTech), Nanjing 211816, P. R. China

[4] Department of Chemistry, Tsinghua University, Beijing 100084, P. R. China

[5] CNRS, CEMHTI UPR3079, Université Orléans, 45071 Orléans, France

[6] College of Materials Science and Engineering, Sichuan University, Chengdu 610065, P. R. China

[7] Institut Universitaire de France, 75005 Paris, France

[†] These authors contributed equally: Hui Shao, Kui Xu

* Correspondence: simon@chimie.ups-tlse.fr (P. Simon)

EXPERIMENTAL SECTION

$Ti_3C_2T_x$ electrode preparation. $Ti_3C_2T_x$ was prepared by removing the Al atom layers from the Ti_3AlC_2 MAX phase (400 mesh, purchased from Carbon-Ukraine Ltd.) in an etching solution of HCl and LiF, which similar to previously reported.[1] Specifically, 2 g LiF salt (Fisher, 98.5%) dissolved in 40 ml of 9 M HCl (Fisher) was served as the etchant, then 2 g of Ti_3AlC_2 powder was slowly added into etchant. After string 48 h at 35 ^oC water bath, the obtained multiple-layer $Ti_3C_2T_x$ suspension was centrifugated and washed with deionized water for several times until the suspension pH reaches 6. Then, the delamination of $Ti_3C_2T_x$ was achieved by sonication for 1 h in an ice bath, with the bubbling of N_2 gas. Afterward, the obtained mixture was centrifugated for 1 h at 3500 r.p.m. The dark supernatant was collected and dried via a freeze-drying method. The obtained $Ti_3C_2T_x$ powder was mixed with deionized water and used for preparing freestanding $Ti_3C_2T_x$ electrode by using a vacuum-filtering process. The thermal treatment used for 500-MXene and 600-MXene film was performed in an Ar atmosphere with a rate of 10 ^oC min^{-1}, a high-power fan was used to cool down the system when the final temperature was reached.

Electrochemical measurements. The electrochemical performances of MXene electrodes were conducted using 3-electrodes Swagelok cell, where 10 mm-diameter disks of freestanding $Ti_3C_2T_x$ films (mass-loadings around 1.9 to 2.1 mg cm^{-2}) as working electrodes, Hg/Hg_2SO_4 as the reference electrode, and over-capacitive YP50F film as the counter electrode. 3 M H_2SO_4 was used as the electrolyte. Electrochemical tests were recorded by a VMP3 potentiostat (Biologic). After pre-cycling at 50 mV s^{-1} for 50 cycles, the cells were tested from the scan rate from 50 to 1000 mV s^{-1}. EIS measurements were recorded in 10 mHz to 100 kHz frequency range with a potential amplitude of 10 mV.

Capacitance and capacity calculations. The capacitance of $Ti_3C_2T_x$ electrode was calculated using:

$$C = \frac{\int_0^t |i|\, dt}{V\, m} \quad (1)$$

$$Q = \frac{C\, V}{3.6} \quad (2)$$

$$t = \frac{V}{s} \quad (3)$$

where C is the gravimetric capacitance (F g^{-1}), Q is the gravimetric capacity (mAh g^{-1}), V is the potential window (V), t is the recording time (s), i is the response current (A), m is the mass of the working electrode (g), and s is the scan rate (V s^{-1}).

Material characterizations. XRD and *in situ* HT XRD patterns of $Ti_3C_2T_x$ films were recorded by D4 and D8 diffractometer (Bruker, Germany), respectively, using a Cu Kα radiation. *In situ* HT XRD measurements were performed under the N_2 atmosphere (100 ml min^{-1}), with an annealing treatment up to 600 ^oC at a rate of 10 ^oC min^{-1}. At each step, the temperature was held at certain values (e.g., 100 ^oC, 200 ^oC, etc.) for recorded the XRD patterns. TPD-MS measurement was conducted under the Ar atmosphere (100 ml min^{-1}). $Ti_3C_2T_x$ film was placed in a thermo-balance and heat up to 1200 ^oC at a rate of 10 ^oC min^{-1}. The resulted decomposition products were monitored by online mass spectrometry (Skimmer, Netzsch, Germany). SEM images were made using a FEG-SEM (Jeol JSM 6700F, Japan). Raman spectra were collected on a LabRAM HR Evolution (HORIBA Jobin Yvon, France) Raman microscope with a 532 nm laser.

***In situ* X-ray absorption spectroscopy (XAS):** *In situ* Ti K-edge XAS measurements were performed on the DiffAbs beamline at synchrotron SOLEIL (France). The electron current of the storage ring was 100 mA, avoiding the beam damage to the sample. The XANES spectra were acquired using a Si(111) double-cam monochromator with an energy resolution of 0.5 eV at Ti K-edge and an energy step of 0.2 eV (from 4961 to 5300 eV). The energy calibration was ensured by measuring a Ti foil, and an internal calibration was done using glitches coming from the Si(111). The incident photons were detected using a first ionization chamber filled with an appropriate gas mixture. A 4-elements silicon drift detector Vortex with an applied ROI was used to select the Ti K_α fluorescence photons, using 4 layers of aluminum foils in order to reduce the counting deadtime. A 3-electrodes cell in PTFE (Zahner) was placed at 80° respect to the incident beam and filled with 1 M H_2SO_4 as electrolyte. Kapton tape with deposited P-$Ti_3C_2T_x$ MXene served as the working electrode, over-capacitive YP50F film and Ag/AgCl as the counter and reference electrode, respectively. MXene electrode was held on each desire potential controlled by a VMP3 potentiostat (Biologic) for 5 mins prior to collect *in situ* XANES spectra.

Electrochemical quartz crystal microbalance (EQCM) measurements. For sample preparation of EQCM, BioLogic 1-in.-diameter Au-coated quartz crystals (oscillating frequency, f_0, 5 MHz) were coated using a precise pipette (Gilson PIPETMAN Classic P20) with a slurry containing 80 wt.% of active material MXene powder, 20 wt.% of polyvinylidene fluoride (Arkema) binder in N-Methyl-2-pyrrolidone (Sigma-Aldrich). The coated quartz crystal was placed on a PTFE holder in which the coated side is orientated toward the reference, and the counter electrode served as the working electrode in a 3-electrode set-up. The counter electrode is a platinum wire. The Hg/Hg_2SO_4 was used as a reference electrode placed between working and counter electrodes. Three electrodes were set in a glassware and immersed in 3 M H_2SO_4 aqueous electrolytes. All the EQCM electrochemical measurements were carried out by a Maxtek RQCM system combined with Autolab PGSTAT101 was used for simultaneous EQCM and electrochemical measurements.

The EQCM data was treated based on the Sauerbrey equation:

$$\Delta m = -C_f \, \Delta f \tag{4}$$

where Δm is the change of mass of the coating and C_f is the sensitivity factor of the crystal. The sensitivity factor of the coated quartz was obtained by performing a copper deposition experiment conducted in 0.1 M $CuSO_4$ mixed with 1 M H_2SO_4 by applying a constant current of 5 mA for 120 seconds. In this experiment, the C_f was calculated to be 14 $ng \cdot Hz^{-1}$ (or 11.02 $ng \cdot Hz^{-1}cm^{-2}$ taking into account the Au crystal electrode surface of 1.27 cm^2). For consistent results, few cycles were run before starting EQCM measurements, to start from stable, reproducible electrochemical signatures.

Simulation Method The simulation system is constituted by MXene electrode layers and 3 M H_2SO_4 aqueous electrolyte. The dynamic and structural properties of two kinds of MXene (P-MXene and 500-MXene) electrode and aqueous electrolytes are detailed studied. Four layers of MXene layer were constructed and immersed into the 3 M H_2SO_4 electrolyte, the schematic figure of the simulation system could be found in Figure S8. The size of the simulation cell is 120.0 × 40.0 × 100.0 $Å^3$ and the periodic boundary condition (PBC) is set in all three directions. Different initial *c*-LPs were set at the initial state, and the MXene electrode layer were all kept free during the simulation. Five Videos (No.1 to 5) attached in the associated content give the parts of trajectories of P-MXene and 500-MXene models. Specifically, video No.1 to 3 gives

side-view of the trajectory of: P-MXene model without water in-between MXene layers, P-MXene model with water in-between MXene layers, 500-MXene with water in-between layers. Video No.4 to 5 gives top-view of water in-between two P-MXene layers, top-view of water in-between two 500-MXene layers, respectively.

The simulations are performed with LAMMPS molecular dynamics code package[2] and the ClayFF force field is employed to determine the interaction between the atoms.[3] The relevant force field parameters could be found in the previous work.[4-6] Canonical ensemble (NVT) with 300 K target temperature is utilized. The particle-particle particle-mesh scheme in k-space is utilized to calculate the long-range electrostatic interactions. All simulations are simulated with a long enough time 3 ns to ensure the structure could adequately converge.

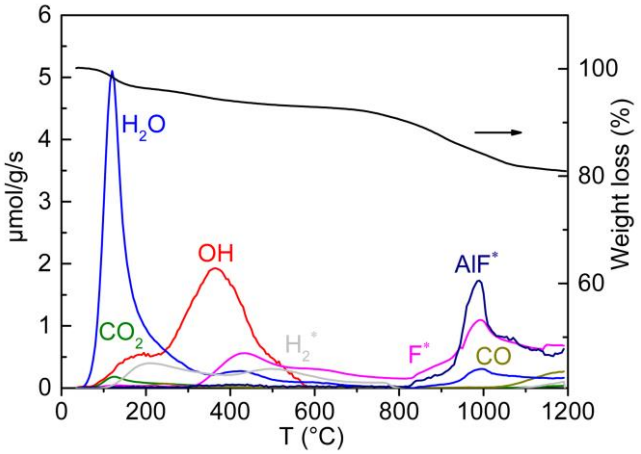

Figure S1. TPD-MS measurements in the temperature range up to 1200 °C. Species marked with asterisks were other gases for $Ti_3C_2T_x$ MXene samples, where no quantification was possible because of the lack of standards.

Table S1. TPD-MS analysis of P-MXene at temperature range up to 1200 °C.

	H_2O µmol/g	H_2O wt.%	-OH µmol/g	-OH wt.%	CO µmol/g	CO wt.%	CO_2 µmol/g	CO_2 wt.%
$Ti_3C_2T_x$	2521	4.5	1626	2.8	238	0.7	187	0.8

As shown in Figure S1, a very small amount of CO_2 formation (0.8%) was observed at a lower temperature range (< 400 °C), as also observed in previous reports[7-8], which could be ascribed to the partial oxidation of C during the etching process.

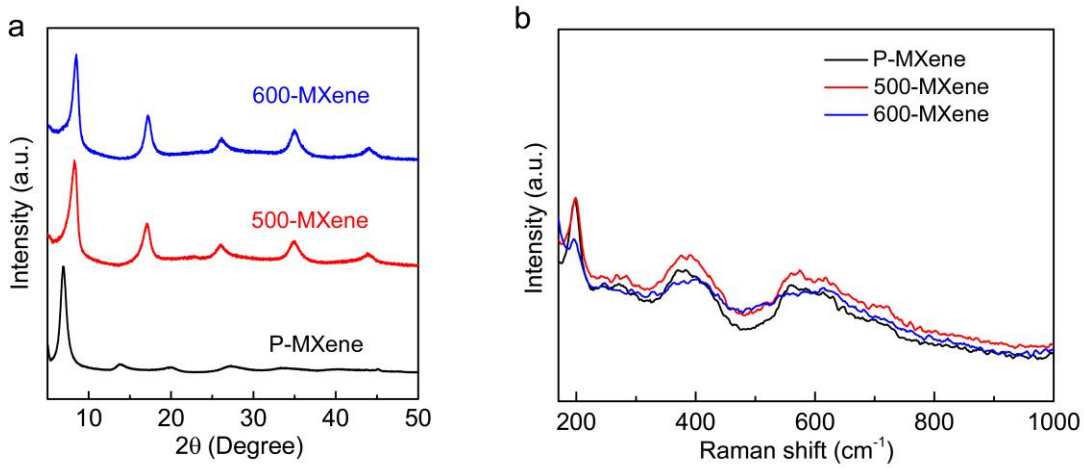

Figure S2. XRD patterns (a) and Raman tests (b) of P-MXene, 500-MXene, and 600-MXene.

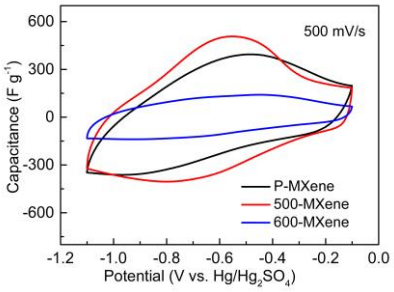

Figure S3. CV profiles of three MXenes at a scan rate of 500 mV s^{-1} in 3 M H_2SO_4.

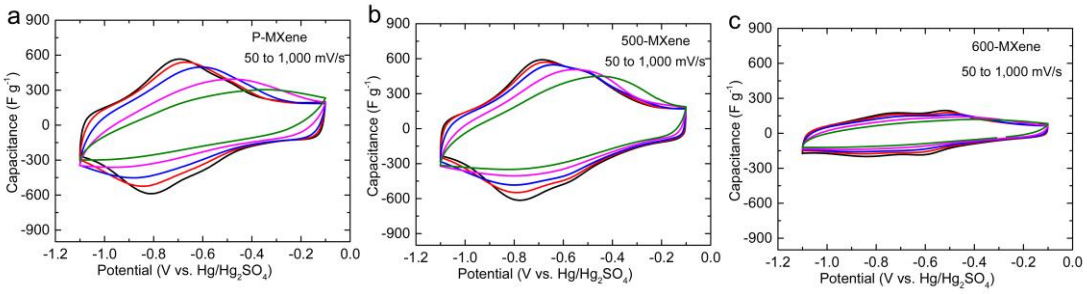

Figure S4. CV profiles at a scan rate range of 50 to 1000 mV s^{-1} in 3 M H_2SO_4 for (a) P-MXene, (b) 500-MXene, and (c) 600-MXene.

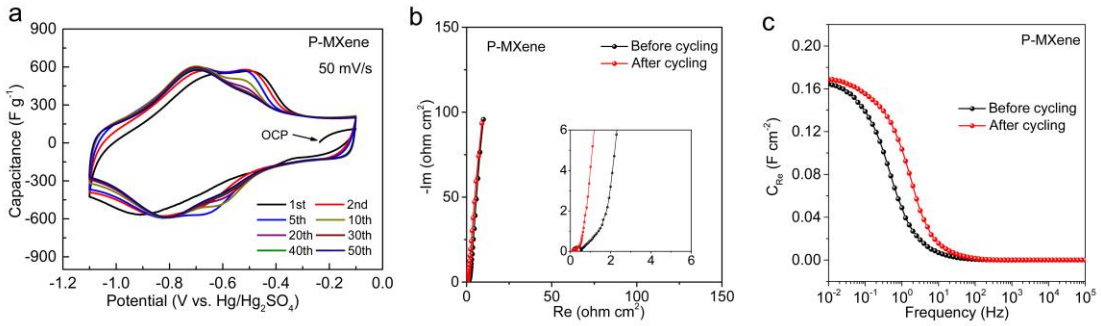

Figure S5. (a) Initial 50 CV cycles of P-MXene at a scan rate of 50 mV s^{-1}. (b) Nyquist plots of Pristine-MXene at OCP before (black) and after (red) electrochemical cycling. (c) Real part of the capacitance calculated from EIS data. All electrochemical tests were recorded in 3 M H_2SO_4.

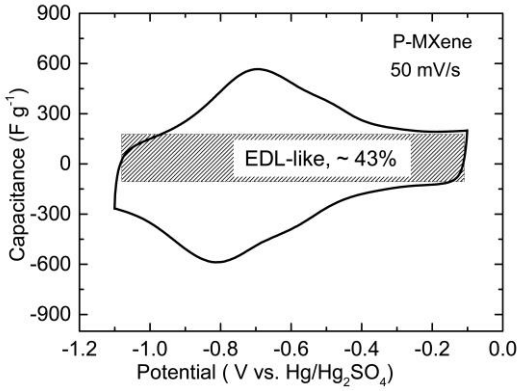

Figure S6. CV profile of P-MXenes at a scan rate of 50 mV s^{-1} in 3 M H_2SO_4. The shaded part indicates the estimated proportion of charge stored by EDL-like mechanisms, accounts for 43% of the total charge, which leaves 57% of the total charge related to the change oxidation state change of Ti.

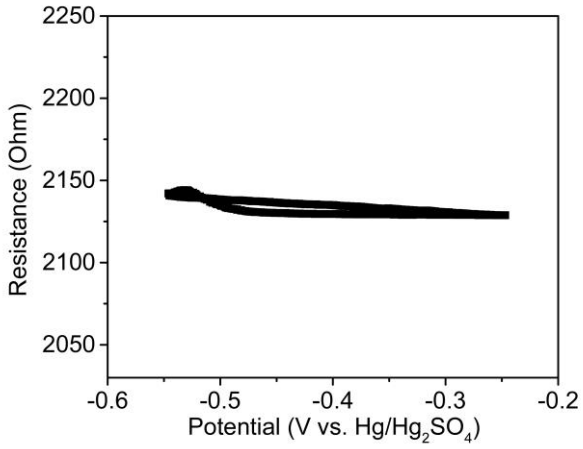

Figure S7. Change of the motional resistance of Pristine-MXene on a gold substrate in 3 M H_2SO_4 at 10 mV s^{-1}. The maximum change of the motional resistance is less than 0.7%, which indicates no influence on the recorded mass change during the EQCM test.

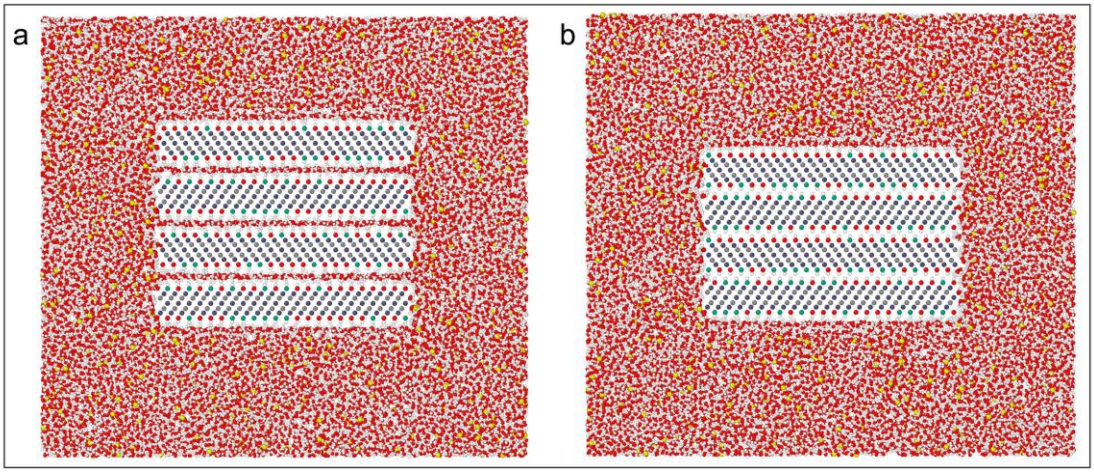

Figure S8. Schematic representation of the simulation model, inner four layers were P-MXene: (a) equilibrium *c* lattice parameter = 26.7 Å with one layer of water in-between, (b) equilibrium *c* lattice parameter = 20.3 Å without water between the layer.

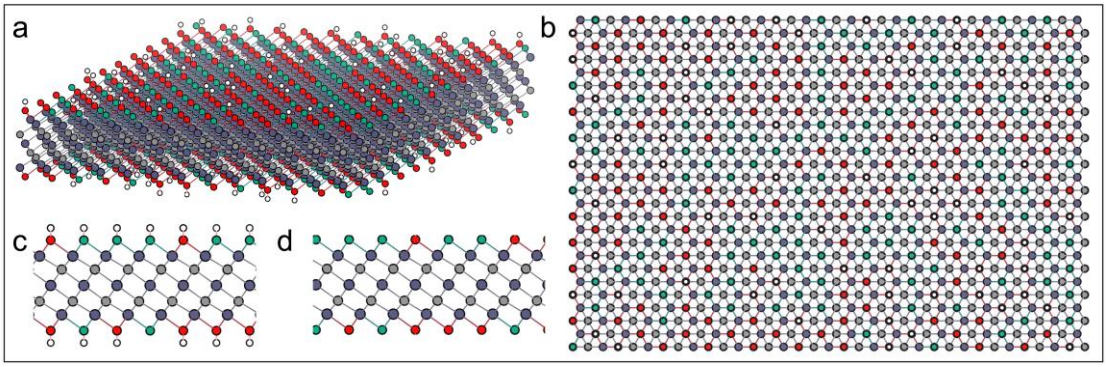

Figure S9. Oblique view (a) and Top view (b) of one P-MXene layer, the different functional groups were randomly placed on the surface, (c) Side view of part of Pristine-MXene layer, (d) Side view of part of the 500-MXene layer.

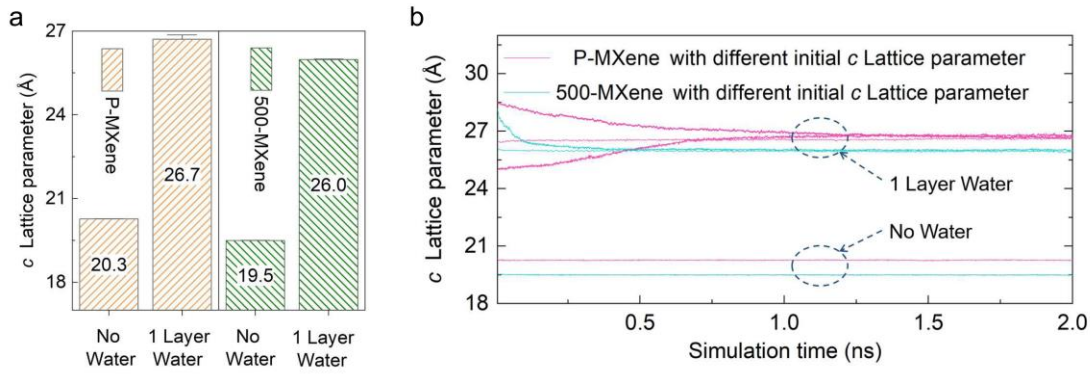

Figure S10. (a) The simulated equilibrium *c* lattice parameters of MXenes with and without water molecules in-between MXene layers. (b) Change of *c* lattice parameters of P-MXene and 500-MXene during the simulation process. Different *c* lattice parameters were set at the beginning of the simulation.

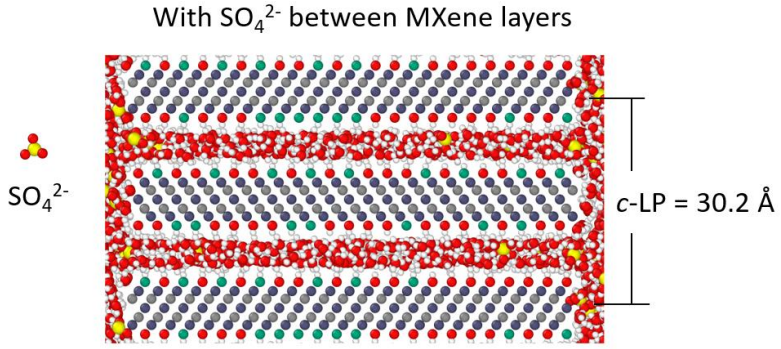

Figure S11. The MD simulated equilibrium c lattice parameter of MXenes with SO_4^{2-} in-between MXene layers.

We assume the expansion of interlayer space results from the H_2O intercalation – instead of H^+ or sulfate intercalation - based on the following reasons. First, the proton radius is around 0.833 fm,[9] which is too small to cause any measurable change of interlayer space during the intercalation/deintercalation process. Differently, the bare and hydrated SO_4^{2-} ion size of SO_4^{2-} is 4.4 Å and 7.6 Å, respectively.[10] According to our MD simulation as well as previous DFT simulation work[11], the thickness of a $Ti_3C_3T_x$ monolayer is around 9.1 Å. As shown in Figure R1, the c-LP reaches 30.2 Å when SO_4^{2-} intercalated between MXene layers, while our XRD measurements show a c-LP of 27.5 Å. Those results evidence that the SO_4^{2-} intercalation is unlikely to occur in our case. Moreover, another previous report[12] studied how anion adsorption affects the interlayer space of MXenes. In this work[12], MXene etching was achieved using a high H_2SO_4 concentration electrolyte mixed with HF, resulting in H_2SO_4-intercalated MXenes with a c-LP of 38 Å. This also indicated that the intercalation of SO_4^{2-} anions lead to larger c-LP (>30 Å) than our current value (27.5 Å). In addition, in our EQCM test, we observed an average molecular weight per charge of around 14 g mol^{-1} during the negative charging process, very close to the molecular weight of hydronium H_3O^+ (19 g mol^{-1}). This also strongly supports the intercalation of H_3O^+ during the cathodic electrochemical process.

Reference

1. Ghidiu, M.; Lukatskaya, M. R.; Zhao, M.-Q.; Gogotsi, Y.; Barsoum, M. W., Conductive two-dimensional titanium carbide 'clay'with high volumetric capacitance. *Nature* **2014,** *516* (7529), 78-81.
2. Plimpton, S., Fast Parallel Algorithms for Short-range Molecular Dynamics. *Journal of Computational Physics* **1995,** *117* (1), 1-19.
3. Cygan, R. T.; Liang, J.-J.; Kalinichev, A. G., Molecular Models of Hydroxide, Oxyhydroxide, and Clay Phases and the Development of a General Force Field. *The Journal of Physical Chemistry B* **2004,** *108* (4), 1255-1266.
4. Xu, K.; Ji, X.; Zhang, B.; Chen, C.; Ruan, Y.; Miao, L.; Jiang, J., Charging/Discharging Dynamics in Two-Dimensional Titanium Carbide (MXene) Slit Nanopore: Insights from molecular dynamic study. *Electrochimica Acta* **2016,** *196*, 75-83.
5. Xu, K.; Lin, Z.; Merlet, C.; Taberna, P.-L.; Miao, L.; Jiang, J.; Simon, P., Tracking Ionic Rearrangements and Interpreting Dynamic Volumetric Changes in Two-Dimensional Metal Carbide Supercapacitors: A Molecular Dynamics Simulation Study. *ChemSusChem* **2018,** *11* (12), 1892-1899.
6. Muckley, E. S.; Naguib, M.; Wang, H.-W.; Vlcek, L.; Osti, N. C.; Sacci, R. L.; Sang, X.; Unocic, R. R.; Xie, Y.; Tyagi, M., Multimodality of structural, electrical, and gravimetric responses of intercalated MXenes to water. *ACS nano* **2017,** *11* (11), 11118-11126.
7. Li, Y.; Shao, H.; Lin, Z.; Lu, J.; Liu, L.; Duployer, B.; Persson, P. O.; Eklund, P.; Hultman, L.; Li, M., A general Lewis acidic etching route for preparing MXenes with enhanced electrochemical performance in non-aqueous electrolyte. *Nature Materials* **2020**, 1-6.
8. Seredych, M.; Shuck, C. E.; Pinto, D.; Alhabeb, M.; Precetti, E.; Deysher, G.; Anasori, B.; Kurra, N.; Gogotsi, Y., High-Temperature Behavior and Surface Chemistry of Carbide MXenes Studied by Thermal Analysis. *Chemistry of Materials* **2019,** *31* (9), 3324-3332.
9. Bezginov, N.; Valdez, T.; Horbatsch, M.; Marsman, A.; Vutha, A.; Hessels, E., A measurement of the atomic hydrogen Lamb shift and the proton charge radius. *Science* **2019,** *365* (6457), 1007-1012.
10. Kerr, J. A., CRC handbook of chemistry and physics. *CRC Press: Boca Raton, FL* **2000,** *2001*, 9-51.
11. Sun, Y.; Zhan, C.; Kent, P. R.; Naguib, M.; Gogotsi, Y.; Jiang, D.-e., Proton Redox and Transport in MXene-Confined Water. *ACS Applied Materials & Interfaces* **2019,** *12* (1), 763-770.
12. Voigt, C. A.; Ghidiu, M.; Natu, V.; Barsoum, M. W., Anion Adsorption, Ti3C2T z MXene Multilayers, and Their Effect on Claylike Swelling. *The Journal of Physical Chemistry C* **2018,** *122* (40), 23172-23179.